ELSEVIER

Journal of Chromatography A, 837 (1999) 35–50

JOURNAL OF CHROMATOGRAPHY A

Monolithic columns containing sol–gel bonded octadecylsilica for capillary electrochromatography

Qinglin Tang, Baomin Xin, Milton L. Lee*

Department of Chemistry and Biochemistry, Brigham Young University, Provo, UT 84602-5700, USA

Received 3 November 1998; received in revised form 6 January 1999; accepted 7 January 1999

Abstract

A new method for preparing monolithic capillary columns is reported. A fused-silica capillary packed with porous octadecylsilica (ODS) particles using a CO_2 slurry was partially filled with a siliceous sol formed by hydrolysis and polycondensation of tetramethoxysilane and ethyltrimethoxysilane. After gelling and aging of the siliceous sol at room temperature, the column was dried with supercritical CO_2. The scanning electron micrograph of a cross-section of the capillary column revealed that the ODS particles were bonded to each other and to the column inner wall by the sol–gel, forming a monolith.

The performance of the monolithic column was evaluated for capillary electrochromatography using small aromatic compounds and polycyclic aromatic hydrocarbons with Tris buffer in aqueous acetonitrile mobile phase. The electroosmotic flow velocity increased with a decrease in Tris buffer concentration from 10 to 5 m*M*. The electroosmotic flow velocity increased significantly with an increase in Tris buffer pH from 5 to 7.5, and then remained nearly constant with Tris buffer pH between 7.5 to 9.0. The electroosmotic flow velocity increased with an increase in acetonitrile content from 20 to 50%, and then remained nearly constant with acetonitrile content between 50 to 90%.

No bubble formation was observed during CEC operation, and all of the test compounds eluted as symmetrical peaks. The logarithms of the retention factors of the aromatic compounds and polycyclic aromatic hydrocarbons decreased linearly with an increase in acetonitrile content. For a 21/29 cm×75 μm I.D. monolithic column containing 9% sol–gel bonded 5 μm ODS, approximately 2.7×10^4 theoretical plates (plate height 7.8 μm; 1.3×10^5 theoretical plates per meter) were measured. It was found that the resistance to mass transfer of unretained thiourea was small, which was attributed to partial filling of the small pores in the particulate packing and partial filling of the interstitial space by the porous sol–gel network. The procedure for column fabrication was simple, and three columns were prepared without failure.

Keywords: Capillary electrochromatography; Sol–gel; Monolithic columns; Octadecylsilica; Column technology

1. Introduction

Capillary electrochromatography (CEC) has emerged as an ultrahigh efficiency liquid-phase separation technique [1–7] due to the plug-like flow profile that originates from electroosmotic flow. Most CEC has been carried out using packed capillary columns of 50–100 μm I.D. packed with 1.5–5 μm diameter packing materials [1–8]. The packing materials are usually retained in the column by two on-column end-frits prepared by sintering packing material [6,9] or silica gel in situ [10] at ends of the

*Corresponding author.

0021-9673/99/$ – see front matter
PII: S0021-9673(99)00057-6

packed bed. Various problems have been observed with typical packed capillary columns in CEC. It is very difficult to reproducibly prepare a highly permeable and mechanically strong end-frit by sintering. Furthermore, the sintering process often generates nonuniformity of the packing bed and gaps next to the end-frits. The intense heat used in the sintering process also partially destroys the stationary phase and, thus, results in active sites in the end-frits. The charged particles may migrate when a high electric field is applied to the column ends, resulting in gaps in the column bed after a period of operation. The nonuniformity of the packing bed, the gaps in the column, and the active sites in the end-frits lead to the formation of bubbles in the capillary during use, which causes irreproducibility in migration times, noisy detector baseline, or even total current breakdown. In order to avoid problems associated with packed capillaries, open tubular columns have been used in CEC [11–13]. However, the low phase ratio and, thus, low sample capacity of an open tubular column makes detection of peaks difficult.

Recently, monolithic columns containing a wall-supported continuous porous bed have shown great potential for CEC due to the inherent advantages of high sample capacity, high column bed stability, and absence of end-frits [14–28]. Three approaches have been employed to prepare monolithic columns. The first is to polymerize an organic monomer in the capillary tubing in situ to form a continuous polymeric bed [14–20]. A desirable selectivity can be achieved by carefully selecting monomers which are commercially available or synthesized in the laboratory. Efficiencies as high as 1.2×10^5 theoretic plates per meter in CEC were obtained with a rigid monolithic column containing a copolymer bed of acrylamide and methacrylate [15]. However, polymeric columns could suffer from solvent swelling or heat deformation although the rigid polymeric monolithic columns minimize these effects.

The second approach is to form a silica-based network in situ using a sol–gel process and then functionalize the network [21–25]. The sol–gel process involves the hydrolysis and polycondensation of precursors such as tetramethoxysilane in a solvent or solvent mixture at a certain pH, followed by drying the resultant wet gel using heat. A silica-based gel network offers high permeability and good heat and solvent resistance. However, the silica gel network suffers from shrinking and/or cracking during drying, which results in poor efficiency and even complete column failure. To alleviate the shrinking and cracking of the sol–gel column bed, Dulat et al. [26] recently prepared an ODS loaded sol–gel monolithic column by suspending ODS particles in the sol solution. An efficiency of 80 000 theoretical plates per meter was obtained using a 3 μm ODS loaded sol–gel column. The moderate efficiency of such columns is believed to result from the inhomogeneous loading of ODS in the column.

The third method is to fuse the porous particulate packing materials in a capillary in situ using a sintering process [27,28]. The sintered column bed was reported to be mechanically strong, and an efficiency of 1.25×10^5 theoretic plates per meter in CEC was obtained with a 75 μm I.D. column containing fused 6 μm ODS particles [27]. However, the preparation of the fused monolithic column is laborious. Moreover, the stationary phase is usually destroyed by the applied heat and by the basic solutions used during the sinterization process, and post deactivation and functionalization of the sintered bed are necessary.

Additional research is still required to design new monolithic columns which offer high efficiency, versatility, reproducibility, and success rate. In a previous paper, we described a method to fabricate monolithic columns by in situ crosslinking of polymer-encapsulated packing materials in a capillary column [29]. Evaluation of such columns in solvating gas chromatography showed that the efficiency and permeability of the crosslinked monolithic column were similar to those of conventional packed capillaries.

In this study, a new method for the preparation of monolithic columns using a sol–gel to bond the packing materials in a packed capillary is described, and the properties of such monolithic columns in CEC are characterized.

2. Experimental

2.1. Materials and chemicals

Fused silica capillaries were purchased from Poly-

micro Technologies (Phoenix, AZ, USA). A Lee Scientific Model 600 SFC pump (Dionex, Salt Lake Division, Salt Lake City, UT, USA) was used to pump supercritical CO_2 during column packing and drying. Zero dead-volume stainless steel unions were purchased from Valco Instruments (Houston, TX, USA). Vydac 201HSB5 ODS (5 μm diameter and 90 Å mean pore diameter) was provided by The Separations Group (Hesperia, CA, USA).

Tetramethoxysilane (TMOS) and ethyltrimethoxysilane (ETMOS) were purchased from Gelest (Tullytown, PA, USA). Other chemicals were obtained from Sigma (St. Louis, MO, USA) and Aldrich (Milwaukee, WI, USA). HPLC grade water was purchased from Mallinckrodt Chemicals (Paris, KY, USA). Trifluoroacetic acid (TFA) aqueous solution at pH 2 was prepared by adding TFA to water until the pH reached 2 as measured with a pH meter.

A Tris buffer stock solution was prepared by mixing appropriate volumes of 50 m*M* Tris-base and 50 m*M* Tris–HCl to give the desired pH. The mobile phase was prepared by diluting the stock buffer solution with appropriate volumes of water and acetonitrile to obtain the desired buffer concentration and pH. In this way, the ionic strength of the mobile phase was kept constant. The mobile phase was filtered through a 0.45 μm pore size nitrocellulose filter (Micron Separations, Westborough, MA, USA) and sonicated for 10 min to chase out the dissolved air using a Branson 1210 sonicator (Alltech Associates, Deerfield, IL, USA). The test mixtures of aromatic compounds (benzylalcohol, benzaldehyde, dimethylphthalate, benzophenone, and biphenyl), and polycyclic aromatic hydrocarbons (naphthalene, biphenyl, fluorene, and phenanthrene) were prepared by dissolving an appropriate amount of each pure chemical into a solution of the same composition as the mobile phase.

2.2. Preparation of packed capillaries

A supercritical fluid packing method [30] was used for capillary column packing. In short, one end of a length of fused-silica capillary was connected to a stainless steel vessel into which an approximate amount of the packing material was placed. The other end of the capillary column was connected to a length of restrictor tubing of 25 μm I.D. using a zero dead-volume union in which a stainless steel frit with 2 μm pores (Valco) was placed. The stainless steel frit was used to retain the particles in the capillary, and the restrictor tubing was used to control the packing speed. The stainless steel vessel was connected to an SFC pump, and packing of the capillary column was carried out in a ultrasonic bath at room temperature by increasing the pressure from 5–35 MPa at 1 MPa min^{-1}. Finally the column was conditioned at 35 MPa for 30 min, and then depressurized overnight.

2.3. Preparation of sol–gel bonded monolithic capillary columns

The sol solution was prepared by mixing appropriate amounts of TMOS, ETMOS, methanol, trifluoroacetic acid (TFA), water and formamide. For example, to obtain a 9% (precursors/solution, v/v) sol solution, the following amounts were used: 20 μl TMOS, 20 μl ETMOS, 200 μl methanol, 15 μl TFA aqueous solution at pH 2, and 200 μl formamide. The apparent pH of the solution was approximately 5, measured using a short-range Alkacid pH test paper (Micro Essential Laboratory, NY, USA). The solution was vortexed for 5 min at room temperature using a S/P® vortex mixer (Baxter Diagonostics, Deerfield, IL, USA) and introduced into a packed capillary column to a desired length using a 100 μl PEEK syringe (Unimetrics, Shorewood, IL, USA) mounted on a PHD 2000 syringe pump (Harvard Apparatus, Holliston, MA, USA). The syringe is strong enough for filling 60 cm of capillary column packed with 5 μm ODS with the nonviscous sol solution at a speed of 1 μl/min. The sol filled packed capillary was stored at room temperature for 24 h for the conversion of the sol to a gel, and for aging of the resulting wet gel. Then, the capillary was connected to an SFC pump using a zero dead-volume union and dried using supercritical CO_2 at 80 atm inlet pressure and 40°C for 5 h, 120°C for 5 h, and 250°C for 2 h. Finally, the packing material at the end of the column that was not bonded by the sol–gel was flushed out, leaving a section of unpacked capillary.

A short length of the monolithic column was usually cut off and a gold coating was sputtered on it for observation using a scanning electron microscope

(JEOL JSN 840A). Before installing the column into the CEC instrument, it was thoroughly washed with acetonitrile and mobile phase, and a 5 mm long detection window was made immediately after the column bed by dissolving away the polyimide coating using concentrated ammonium hydroxide.

2.4. CEC experiments

CEC experiments were carried out using a home-made electrochromatograph which is similar to that described by Xin et al. [31]. In short, the electrochromatograph consisted of a CZE1000R 30 kV power supply (Spellman, Plainview, NY, USA) and a Spectra 100 UV detector (Thermoseparation Products, Fremont, CA, USA) with a capillary flow-cell for on-column detection. An SP4290 integrator (Spectra Physics, Fremont, CA, USA) was used for data recording. A model 486 DX computer (PONY Computer, Houston, TX, USA) with home-made control software and an ADIO 1600 A/D card (Industrial Computer Source, San Diego, CA, USA) were used to control the high voltage supply. The column inlet and outlet vials were housed in two home-built CTFE plastic chambers, which were placed in a Plexiglas box for operator safety. The minimum capillary lengths from the column inlet to the detector window and from the window to the column outlet were 20 and 8 cm, respectively. Samples were introduced into the column by electrokinetic injection. Thiourea dissolved in a solution of the mobile phase was used as the EOF marker.

3. Results and discussion

3.1. Column preparation

Fig. 1 shows a scanning electron micrograph of a 9% sol–gel bonded 5 μm ODS monolithic column. The ODS particles were attached to each other and to the capillary wall by the gel network, forming a monolith.

The key to successful column preparation using the sol–gel method is the composition of the sol solution. The sol solution is prepared by mixing appropriate amounts of precursors, solvents, catalyst, and chemical drying agents. In a classical sol–gel process for silica glasses, a single precursor, TMOS, is typically used [32]. Shrinking and cracking of the silica gel fabricated from TMOS alone are often observed during drying, and the gel network is active because of the exposed silanol groups on the gel surface. It was reported that alkyl derivatives of TMOS as a co-precursor with TMOS results in a flexible gel network with a more open pore structure [33], which could alleviate capillary stress during drying. The alkyl groups can also deactivate the gel network by becoming exposed outside the gel network. ETMOS was selected as a co-precursor with TMOS in this study to obtain an open and inert gel network without leading to undesirable high retention for the solutes. In this way, the separation mechanism of the ODS was preserved and the sol–gel only acted as an inert bonding agent. Methanol was used as solvent because of its good solvating ability for the precursors and its high wetting ability for the gel network. TFA was employed as a catalyst in the hydrolysis of the precursors because TFA has low levels of metal ions and is easy to remove. Chemical drying agents, such as formamide and glycerol, are used in classical sol–gel processes to obtain crack-free silica products [32]. In this study, formamide was used as a chemical drying agent. Another role of formamide was to adjust the pH of the sol solution in order to obtain the appropriate gelation time.

The gelation time of the siliceous sol solution depends on the types and amounts of precursors, the type and amount of solvent, the type and amount of catalyst, and the pH of the sol solution [32]. The relationship between gelation time and volume composition of the sol solution is given in Table 1. The gelation time was controlled in this study so that the sol solution could be easily introduced into the packed capillary column.

Although the composition of the sol solution was carefully controlled, only very short lengths of crack-free sol–gel bonded monolithic columns were obtained using a conventional drying process. Cracking of the column bed is believed to result from capillary forces generated during evaporation of the solvent. A supercritical fluid has been used to dry the gel network in order to obtain crack-free gel products because the surface tension of a supercritical fluid is zero [32]. A supercritical fluid dried gel product is

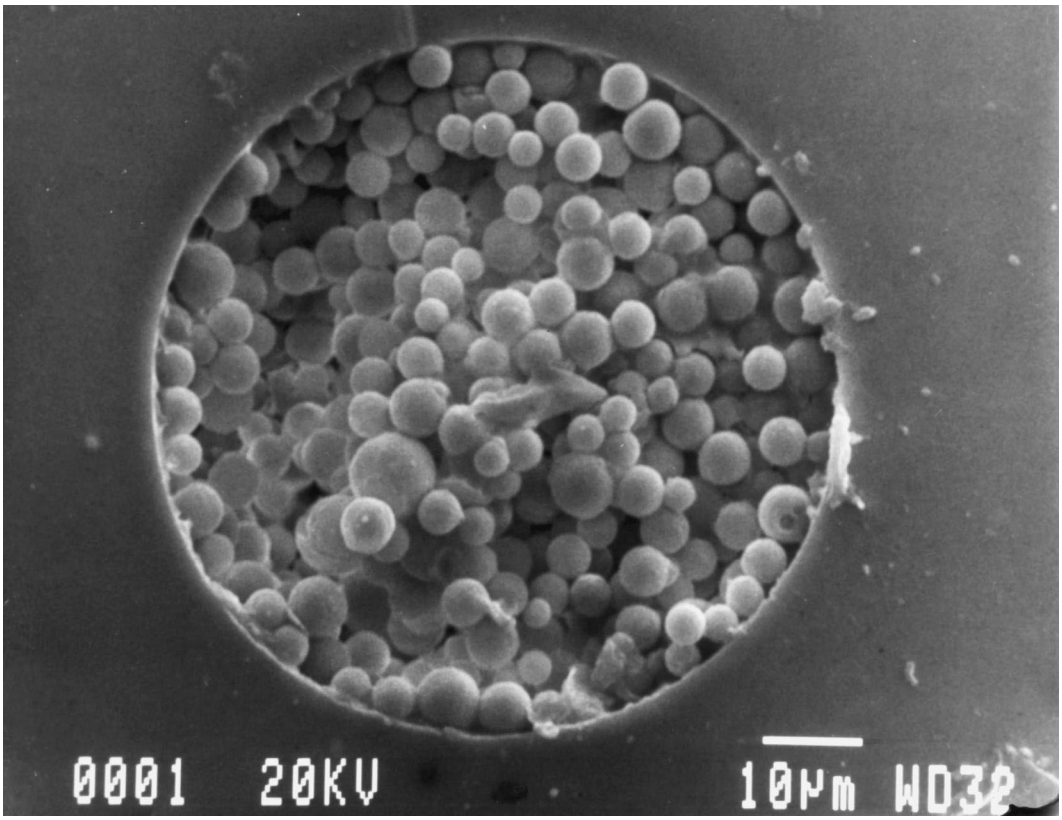

Fig. 1. Scanning electron micrograph of the end of a 75 μm I.D. monolithic column containing 9% sol–gel bonded 5 μm ODS particles.

called an aerogel because it possesses up to 90% porosity [34]. The problem associated with supercritical fluid drying in the fabrication of monolithic columns in the past was that the critical point of the methanol solvent was so high that the stationary phase and even the gel network dissociated in the supercritical fluid. Malik et al. suggested the use of supercritical CO_2 generated in situ by thermal decomposition of ammonium bicarbonate which was incorporated in the sol solution to dry the gel network [25]. This method was found not suitable for our sol–gel bonded ODS monolithic columns because the decomposition of ammonium bicarbonate was difficult to control, and the rapid evolution of CO_2 caused disturbances and gaps in the column bed. In this study, supercritical CO_2 was pumped

Table 1
Relationship between gelation time and volume composition of the sol solution.

Reagent volume (μl)[a]					Gelation time (h)	Visual properties of gel
TMOS	ETMOS	MeOH	TFA	FA		
40	0	200	15 (pH1)	200	14	Transparent
40	0	200	15 (pH2)	200	3	Transparent
0	40	200	15 (pH2)	200	no gel	
20	20	200	15 (pH2)	200	4	Translucent

[a] TMOS = tetramethoxylsilane, ETMOS = ethyltrimethoxylsilane, MEOH = methanol, TFA = trifluoroacetic acid, FA = formamide.

through the column to replace the solvent and residual reactants using a supercritical fluid chromatographic pump, and the column was then dried in supercritical CO_2. It was observed that the resulting sol–gel bonded ODS monolithic columns were crack-free, and three successful columns were prepared with high reproducibility.

3.2. Column mechanical strength and stability

The mechanical strength and permeability of the sol–gel bonded ODS monolithic columns were observed to be dependent upon the volume percentages of the precursors in the sol solution. A high percentage of precursors in the sol solution led to low permeability of the monolithic column, while a low percentage of precursors resulted in a weak gel network. A 9% sol–gel network was a good compromise between mechanical strength and permeability. There was no perceivable change in the column bed under microscope observation after a 24/32 cm×75 μm I.D. 9% sol–gel bonded 5 μm ODS monolithic column was flushed with 80% acetonitrile solution containing 5 m*M* aqueous Tris buffer for 24 h, and the column was used in CEC for 3 weeks.

3.3. Factors affecting electroosmotic flow velocity

The electroosmotic flow (EOF) velocity generated at the surface of a charged bed under an external electric field can be expressed by the Smoluchowski

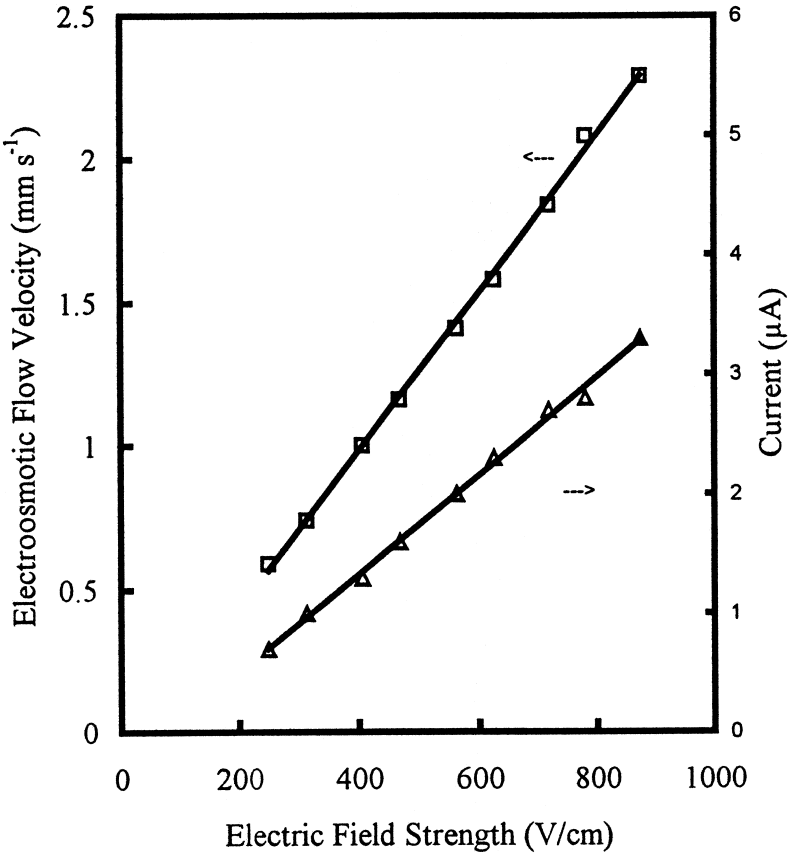

Fig. 2. Plot of electroosmotic flow velocity (□) and current (△) versus applied electric field strength. Conditions: 24/32 cm×75 μm I.D. monolithic column containing 9% sol–gel bonded 5 μm ODS with 90 Å pores, 80% acetonitrile aqueous mobile phase containing 5 m*M* Tris buffer at pH 8.0, 5 kV×2 s electrokinetic injection, 0.3 m*M* thiourea used as EOF marker, 254 nm UV detection.

equation [35] which was derived for an open tube assuming that there is no electrical double layer overlap [2,4]:

$$\nu_{eo} = \frac{L_M}{t_{eo}} = \frac{\varepsilon_0 \varepsilon_r \zeta}{\eta} E \quad (1)$$

where ν_{eo}, L_M, t_{eo} ε_0, ε_r, ζ, and E are the EOF velocity, the length of the column from the column inlet to the detection window, the migration time of the EOF marker, the permittivity of the vacuum, the dielectric constant of the mobile phase, the zeta potential, the viscosity of the mobile phase, and the external electric field strength, respectively. Eq. (1) implies that the EOF velocity depends on the properties of the mobile phase and the applied electric field strength.

3.4. Effect of applied electric field strength

Fig. 2 shows plots of EOF velocity and current versus the applied electric field strength with 80% acetonitrile aqueous mobile phase containing 5 m*M* Tris buffer at pH 8 using thiourea as an EOF marker. As can be seen, the electroosmotic flow increased linearly with an increase in the applied electric field

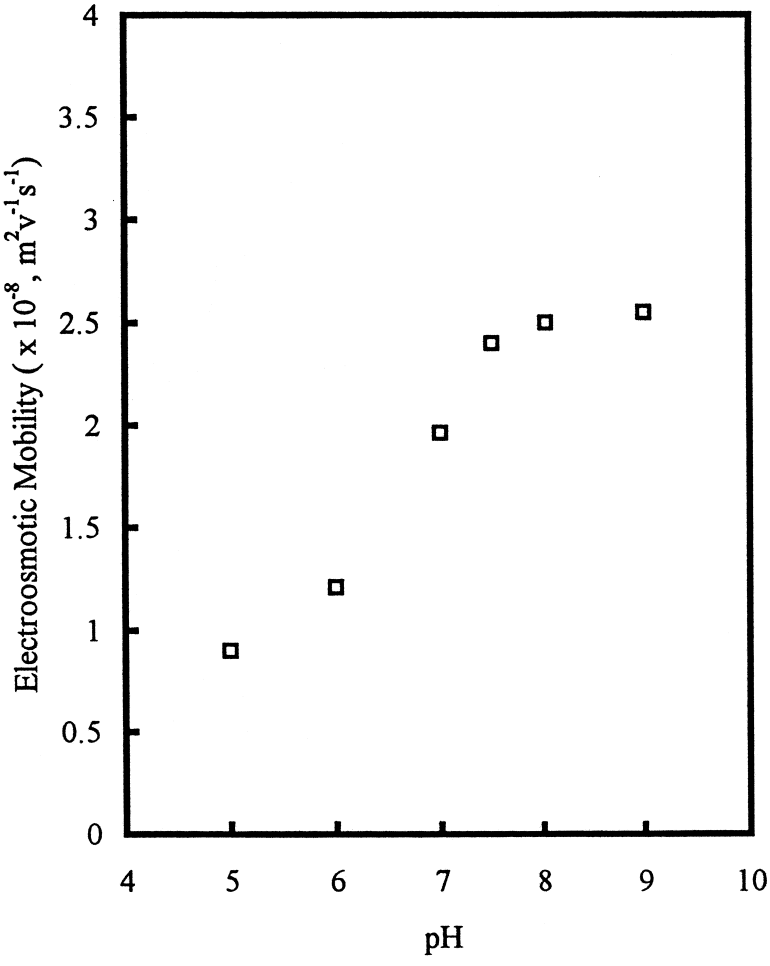

Fig. 3. Plot of electroosmotic mobility versus mobile phase pH. Conditions: 80% (v/v) acetonitrile aqueous mobile phase containing 5 m*M* Tris buffer, 24/32 cm×75 μm I.D. monolithic column containing 9% sol–gel bonded 5 μm ODS with 90 Å pores, 5 kV×2 s electrokinetic injection, 625 V/cm applied electric field strength, 0.3 m*M* thiourea used as EOF marker, 254 nm UV detection.

strength. The magnitude of the EOF velocity in a 24/32 cm×75 μm I.D. 9% sol–gel bonded 5 μm monolithic column was 2.3 mm/s at 875 v/cm applied electric field strength, which is comparable to the linear velocity of mobile phase commonly used in HPLC. Fig. 2 also shows that the current increased linearly with the applied electric field strength, which suggests that Joule heating in the column can be ignored between the electric field strengths of 250 and 875 v/cm under the experimental conditions used in this study.

The electroosmotic mobility instead of the electroosmotic flow velocity should be measured for better understanding of the effect of the mobile phase composition on EOF velocity. The electroosmotic mobility can be expressed by:

$$\mu_{eo} = \frac{\nu_{eo}}{E} = \frac{\delta\sigma}{\eta} \quad (2)$$

where μ_{eo}, δ, and σ are the electroosmotic mobility, the electrical double layer thickness, and the total excess charges per unit area in the stern plane, respectively [11]. E and η are the same as in Eq. (1). The double layer thickness in an aqueous solution is a function of the ionic strength of the solution expressed by:

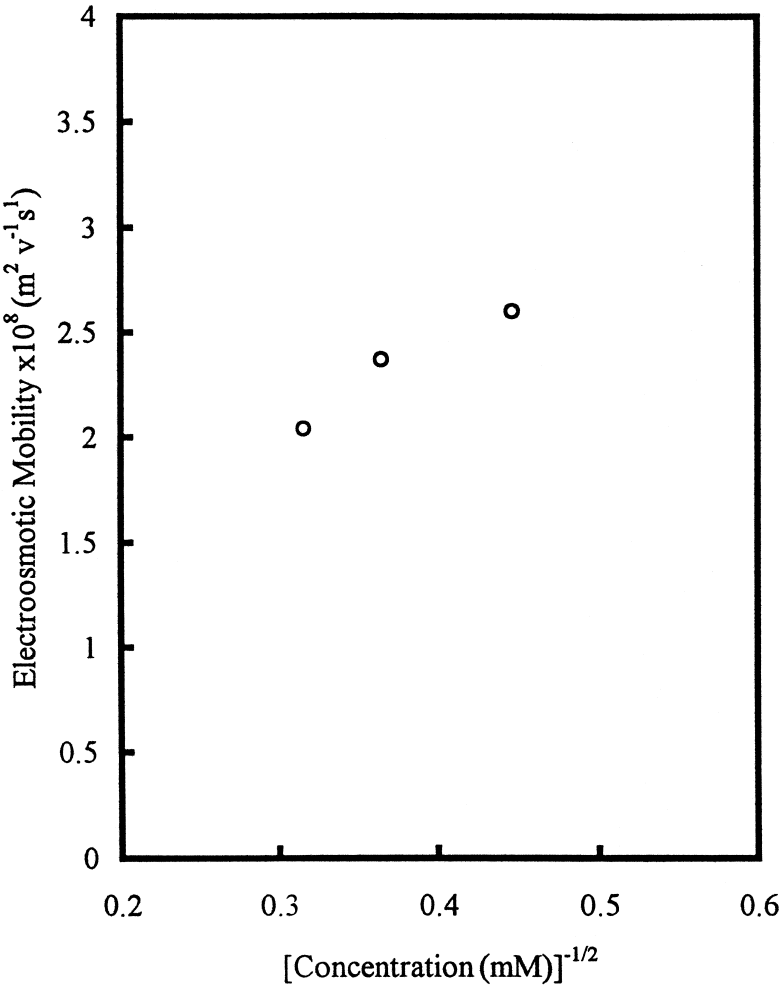

Fig. 4. Plot of electroosmotic mobility versus concentration of Tris buffer in the mobile phase. Conditions: 80% (v/v) acetonitrile aqueous mobile phase containing Tris buffer at pH 8.0, other conditions are the same as in Fig. 3.

$$\delta \cong \frac{1}{3 \cdot 10^{7} |Z| \sqrt{C}} \quad (3)$$

where Z and C are the number of valence electrons, and the buffer concentration, respectively [11]. We studied the effect of factors including pH, concentration of Tris buffer, and acetonitrile content in the mobile phase on the electroosmotic mobility using thiourea as an EOF marker.

3.5. Effect of Tris buffer pH

The effect of buffer pH on electroosmotic mobility was investigated for solutions in 80% acetonitrile and 5 m*M* buffer at different pH values. The pH was adjusted in the aqueous phase prior to the addition of acetonitrile by mixing the appropriate 50 m*M* Tris-base and 50 m*M* Tris–HCl stock solutions. The results are given in Fig. 3. It can be seen that the electroosmotic mobility increased significantly with an increase in the buffer pH from pH 5.0–7.5, and remained nearly constant at pH 7.5–9.0. Ionization of the silanol groups increased with an increase in Tris buffer pH, leading to more total excess charges per unit area in the stern plane and, thus, greater electroosmotic mobility. When the pH was greater than pH 7.5, most of the silanol groups were ionized and the electroosmotic mobility approached a maximum.

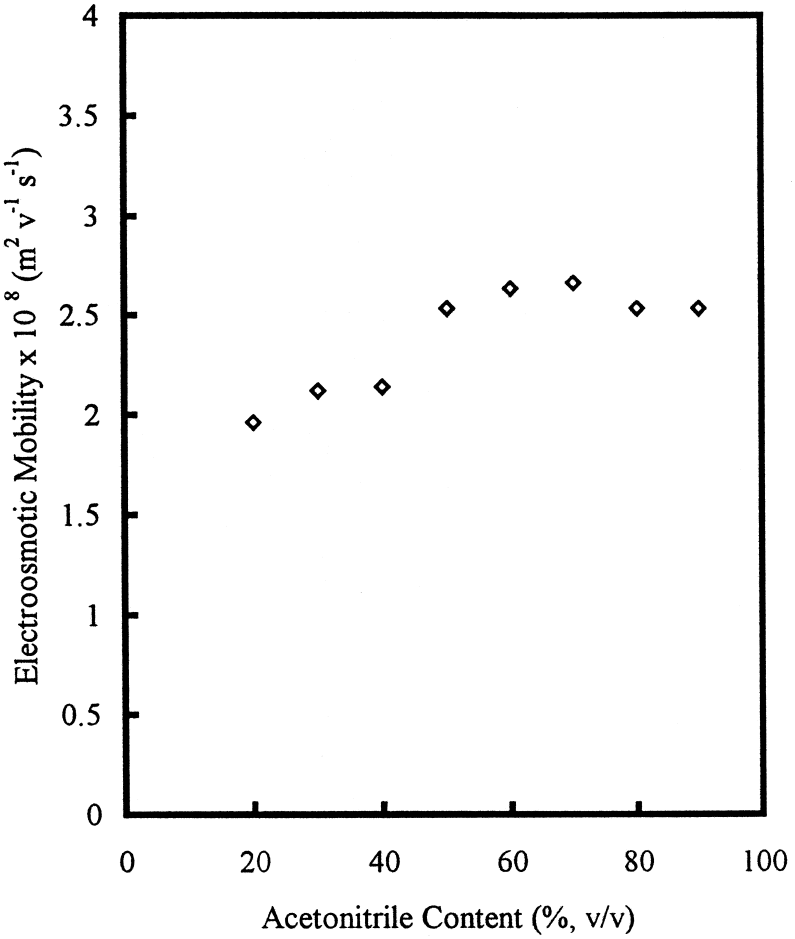

Fig. 5. Plot of electroosmotic mobility versus acetonitrile content in the mobile phase. Conditions: acetonitrile aqueous mobile phase containing 5 m*M* Tris buffer at pH 8.0, other conditions are the same as in Fig. 3.

3.6. Effect of Tris buffer concentration

The effect of buffer concentration on electroosmotic mobility was studied with Tris buffer at pH 8.0 in the range of 5 to 10 m*M* in 80% acetonitrile aqueous solution. The buffer concentration was adjusted by mixing appropriate amounts of 50 m*M* buffer stock solution and water into acetonitrile. Fig. 4 shows a plot of electroosmotic mobility versus the inverse of the square root of the Tris buffer concentration. It can be seen that the electroosmotic mobility decreased with an increase in Tris buffer concentration. However, the linear relationship between the electroosmotic mobility and the inverse of the square root of the Tris buffer concentration as predicted by the zeta potential theory (Eqs. (2) and (3)) was not found, which suggested that Eq. (3) could be not applied for organic aqueous solution.

3.7. Effect of acetonitrile content

The effect of acetonitrile content in the mobile phase on the electroosmotic mobility was investigated by plotting electroosmotic mobility versus acetonitrile content with 5 m*M* Tris buffer at pH 8.0 (Fig. 5). The acetonitrile content was adjusted by mixing appropriate volumes of acetonitrile, water, and buffer to keep a constant ionic strength and pH.

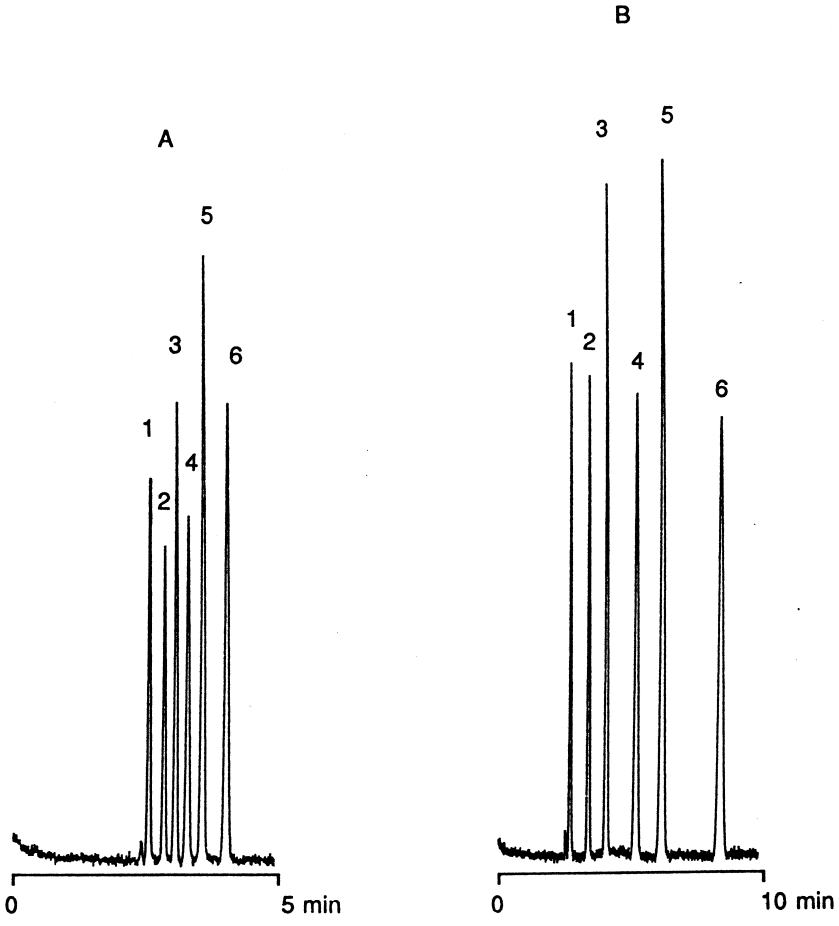

Fig. 6. Electrochromatogram of aromatic compounds. Conditions: 21/29 cm×75 μm I.D. monolithic column containing 9% sol–gel bonded 5–26 μm ODS with 90 Å pores, (A) 80% (v/v) and (B) 60% (v/v) acetonitrile aqueous mobile phase containing 5 m*M* Tris buffer at pH 8.0, 5 kV×2 s electrokinetic injection, 15 kV applied voltage, 254 nm UV detection. Peak identifications: (1) thiourea, (2) benzylalcohol, (3) benzaldehyde, (4) dimethylphthalate, (5) benzophenone, and (6) biphenyl.

Fig. 5 shows that the electroosmotic mobility increased slowly with an increase in acetonitrile content from 20 to 50% and remained nearly constant between an acetonitrile content of 50–90%. There was a sharp increase in the electroosmotic mobility when the acetonitrile content was changed from 40 to 50%, which was also observed for fused ODS monolithic columns [27].

3.8. CEC separation of aromatic compounds and PAHs.

Figs. 6 and 7 show separations of a standard mixture of five aromatic compounds and a standard mixture of four PAHs, respectively. The mobile phase was composed of either 60 or 80% (v/v) aqueous acetonitrile containing 5 m*M* Tris at pH 8.0, and thiourea was used as an unretained marker. It should be mentioned that bubble formation was not observed when using the sol–gel monolithic column with both ends at one atmosphere. The absence of bubble formation in the monolithic column was attributed to the uniform structure of the sol–gel bonded monolithic column bed that was readily wetted by the mobile phase over a wide composition range.

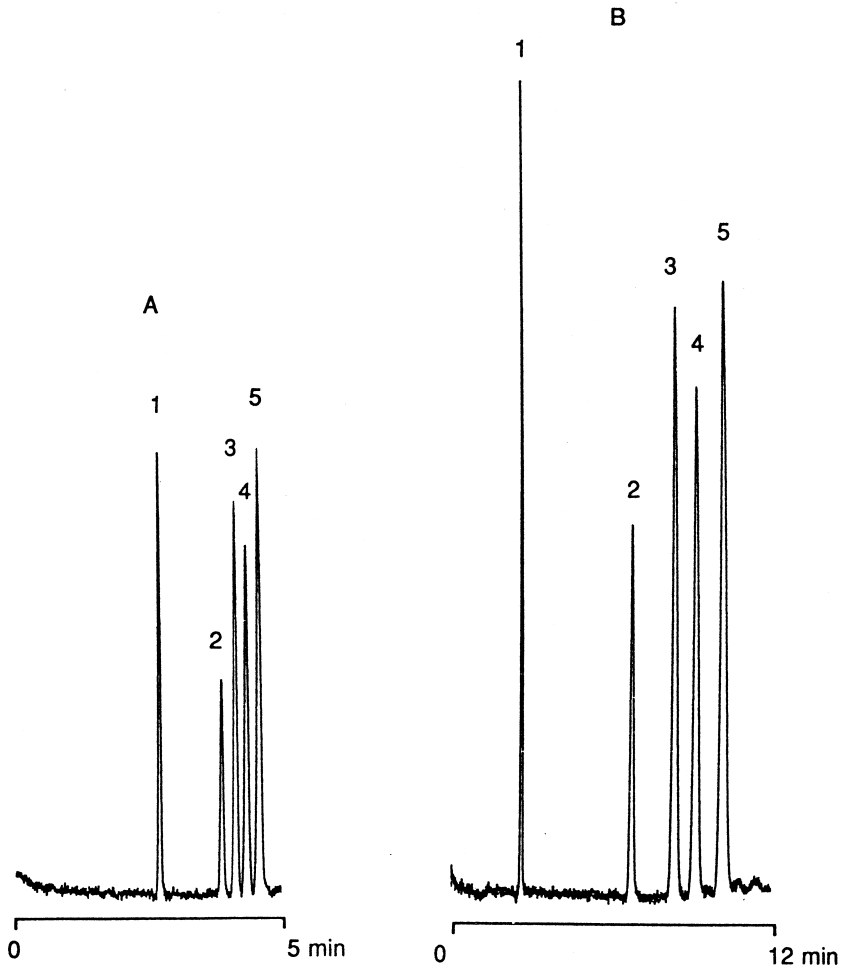

Fig. 7. Electrochromatogram of polycyclic aromatic hydrocarbons. Conditions: (A) 80% (v/v) and (B) 60% (v/v) acetonitrile aqueous mobile phase containing 5 m*M* Tris buffer at pH 8.0, other conditions are the same as in Fig. 6. Peak identifications: (1) thiourea, (2) naphthalene, (3) biphenyl, (4) fluorene, and (5) phenanthrene.

Table 2
Asymmetry factors for chromatographic peaks of aromatic compounds and polycyclic aromatic hydrocarbons[a]

Name	Retention factor	Asymmetry factor
Benzylalcohol	0.22	1.09
Benzaldehyde	0.48	1.05
Dimethylphthalate	0.89	1.06
Benzophenone	1.23	1.04
Naphthalene	1.52	1.03
Biphenyl	2.13	1.04
Fluorene	2.44	1.06
Phenanthrene	2.93	1.07

[a] 60% acetonitrile aqueous mobile phase containing 5 m*M* Tris buffer at pH 8.0, other conditions are the same as in Figs. 6 and 7.

3.9. Characteristics of the sol–gel bonded monolithic columns

Asymmetry factors at 10% peak height are often used to measure peak symmetry [36]. The asymmetry factors for the aromatic compounds measured from Figs. 6 and 7 (60% acetonitrile aqueous mobile phase) are listed in Table 2. All of the peaks had asymmetry factors less than 1.1. Symmetrical peaks for benzylalcohol and benzaldehyde in Fig. 6 suggested that the sol–gel matrix was inert and no post deactivation or functionization of the column bed was necessary. This is a major advantage over fused monolithic columns.

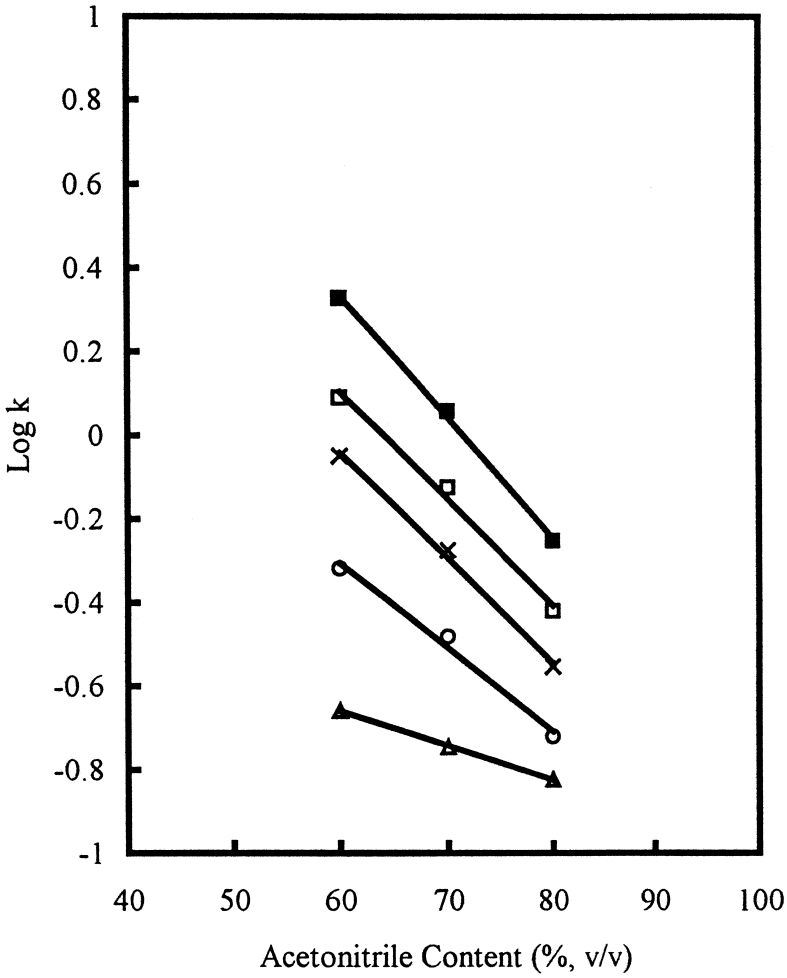

Fig. 8. Plots of the logarithm of retention factors for aromatic compounds versus acetonitrile content in the mobile phase. Conditions: 60–80% acetonitrile aqueous mobile phase containing 5 m*M* Tris buffer at pH 8.0, other conditions are the same as in Fig. 6. (△) benzylalcohol, (○) benzaldehyde, (×) dimethylphthalate, (□) benzophenone, and (■) biphenyl.

Figs. 8 and 9 show plots of the logarithm of retention factors for aromatic compounds and PAHs, respectively, versus acetonitrile content. It can be seen that these plots are linear with negative slopes, typical for reversed-phase separations. The retention factors for naphthalene and phenanthrene were 0.45 and 0.73 at 80% acetonitrile, and 1.52 and 2.93 at 60% acetonitrile, respectively. The relatively small retention factors for PAHs on the sol–gel bonded monolithic column implies that the small pores in the ODS particles could be filled. Comparing the retention factors in Figs. 8 and 9, the slopes of the lines for PAHs and nonpolar aromatic compounds were higher than the slope of the line for benzylalcohol, which is believed to be due to the strong hydrogen bond interaction between benzylalcohol and water in the mobile phase.

Fig. 10 shows a plot of plate height versus EOF velocity as measured for thiourea on a 21/29 cm× 75 μm I.D. monolithic column containing 9% sol–gel bonded 5 μm ODS. Over 2.7×10^4 theoretical plates (plate height 7.8 μm; 1.3×10^5 theoretical plates per meter) for unretained thiourea at an EOF velocity of 1.0 mm/s were measured for this column using 80% acetonitrile aqueous mobile phase containing 5 m*M* Tris buffer at pH 8.0. This efficiency is comparable to those reported for polymeric monolithic columns [15] and fused ODS monolithic columns [27]. The efficiency characteristics of the sol–gel bonded monolithic column were evaluated

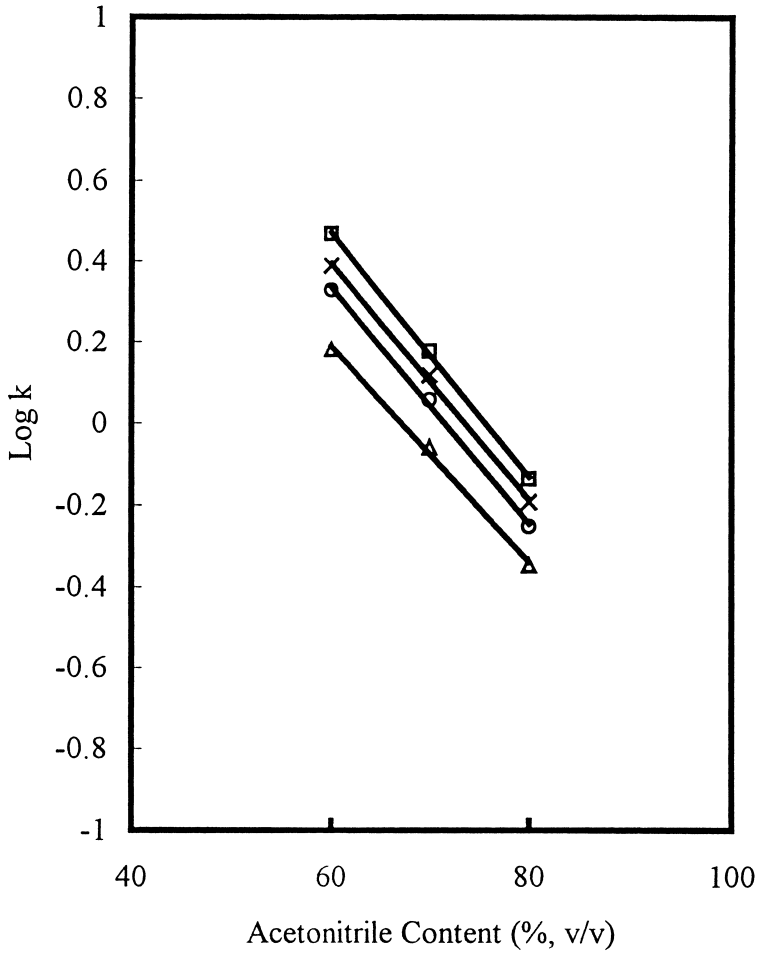

Fig. 9. Plots of the logarithm of retention factors for polycyclic aromatic hydrocarbons versus acetonitrile content in the mobile phase. Conditions: same as in Fig. 8. (△) naphthalene, (○) biphenyl, (×) fluorene, and (□) phenanthrene.

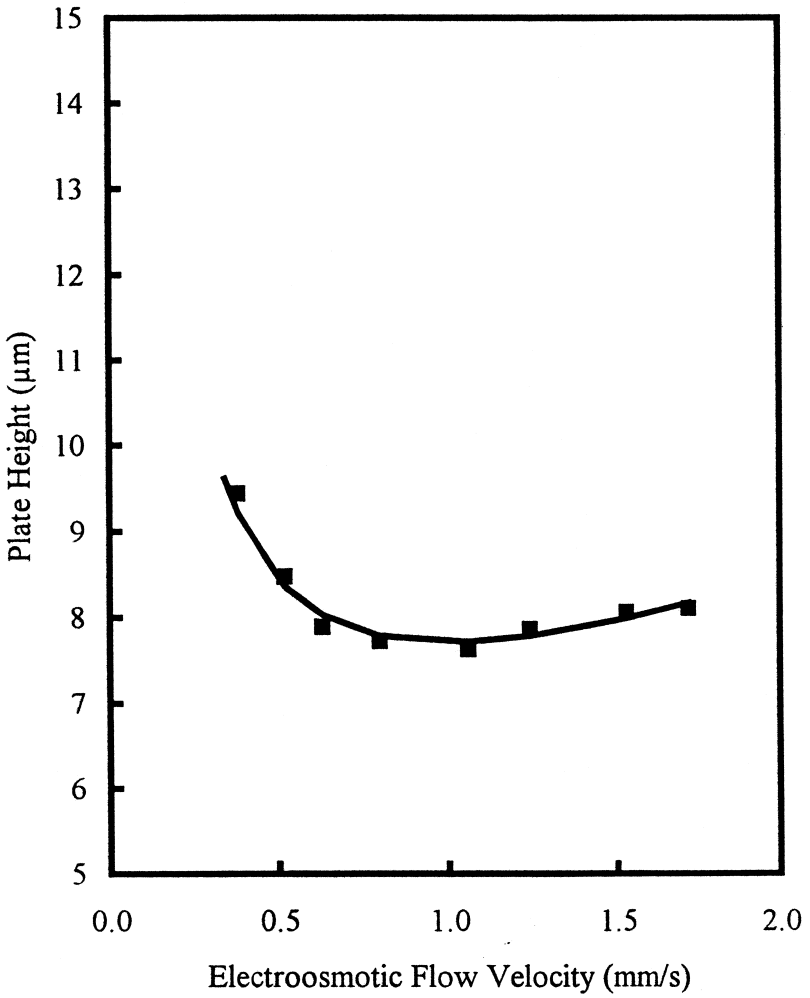

Fig. 10. Plot of plate height versus electroosmotic flow velocity as measured using thiourea. Conditions: 21/29 cm×75 μm I.D. monolithic column containing 9% sol–gel bonded 5 μm ODS with 90 Å pores, 80% (v/v) acetonitrile aqueous mobile phase containing 527 m*M* Tris buffer at pH 8.0, 5 kV×2 s electrokinetic injection, 254 nm UV detection.

(see Table 3) by fitting the efficiency data into the van Deemter equation [36]:

$$H = A + \frac{B}{u} + Cu \quad (4)$$

where H is the plate height and u is the electroosmotic flow velocity. A, B, and C are constants related to the chromatographic system. As can be seen from Table 3, the A term is small, which is due to the plug-like flow profile of the electroosmotic flow. The resistance to mass transfer of the unretained thiourea was 1.5×10^{-3} s, which suggests that

Table 3
Efficiency characteristics for a monolithic column containing 9% sol–gel bonded 5 μm ODS[a]

H_{min} (μm)	7.71
N (plate m^{-1})	1.30×10^{5}
V_{opt} (mm s^{-1})	1.0
A (μm)	4.72
B ($\times10^{3}$ μm^2 s^{-1})	1.49
C (10^{-3} s)	1.5

[a] Chromatographic conditions are listed in the legend for Fig. 10.

Table 4
Reproducibility of retention factors for aromatic compounds and polycyclic aromatic hydrocarbons from run-to-run and column-to-column[a]

Compounds	Run-to-run (Mean±RSD)	Column-to-column (Mean±RSD)
Benzylalcohol	0.11±2.5	0.11±5.8
Benzaldehyde	0.19±2.3	0.19±3.7
Dimethylphthalate	0.28±1.4	0.28±4.1
Benzophenone	0.38±1.6	0.39±4.8
Naphthalene	0.45±1.4	0.46±5.4
Biphenyl	0.55±1.5	0.56±4.0
Fluorene	0.63±3.4	0.64±6.9
Phenanthrene	0.73±1.5	0.74±8.6

[a] 80% acetonitrile aqueous mobile phase containing 5 m*M* Tris buffer at pH 8.0, other conditions are the same as in Figs. 6 and 7.

the small pores in the particles and the void spaces between particles were partially filled by the sol–gel network.

Run-to-run reproducibility was tested by measuring the retention factors of aromatic compounds and PAHs for ten consecutive runs under the same conditions, and column-to-column reproducibility was determined by measuring the retention factors of aromatic compounds and PAHs on three 21/29 cm×75 μm I.D. monolithic columns containing 9% sol–gel bonded 5 μm ODS under the same conditions. These data are listed in Table 4. As can be seen, the run-to-run reproducibilities of retention factors were within 4% relative standard deviation while the column-to-column reproducibilities were within 9% relative standard deviation. It should be mentioned that the CEC instrument was not thermostated, although it was placed in a room with temperature control at roughly 20°C. The good retention factor reproducibility for run-to-run and column-to-column suggests that sol–gel bonded monolithic columns can provide reproducible measurements for routine analysis.

4. Conclusions

A new method for preparing monolithic columns was developed by bonding the packing materials with sol–gel in the capillary in situ. The procedure was simple and reproducible. These sol–gel bonded monolithic columns were stable, inert, highly efficient, and inherited the versatility of commercially available packing materials. These sol–gel bonded monolithic columns are expected to be suitable for nano-HPLC and packed capillary column GC as well as CEC.

Acknowledgements

The authors would like to thank Dr. Paul Kostel (The Separations Group, Hesperia, CA, USA) for providing the Vydac packing materials, and Mr. Samuel E. Tolley for help in building the capillary electrochromatograph. This work was funded in part through collaboration with Sensar/Larson-Davis under a National Science Foundation Small Business Technology Transfer Program, Grant No. DMI-9705341. Partial support was also provided by G.D. Searle, Research & Development Division, Skokie, IL.

References

[1] V. Pretorius, B.J. Hopkins, J.D. Schieke, J. Chromatogr. 99 (1974) 23.
[2] J.W. Jorgenson, K.D. Lukacs, J. Chromatogr. 218 (1981) 209.
[3] J.H. Knox, I.H. Grant, Chromatographia 24 (1987) 135.
[4] J.H. Knox, Chromatographia 329 (1988) 26.
[5] J.H. Knox, I.H. Grant, Chromatographia 32 (1991) 317.
[6] N.W. Smith, M.B. Evans, Chromatographia 38 (1994) 649.
[7] C. Yan, R. Dadoo, H. Zhao, R.N. Zare, D.J. Rakestraw, Anal. Chem. 67 (1995) 2026.
[8] M.M. Dittmann, G.P. Rozing, J. Chromatogr. A 744 (1996) 63.
[9] S.E. van den Bosch, S. Heemstra, J.C. Kraak, H. Hoppe, J. Chromatogr. A 755 (1996) 165.
[10] H.J. Cortes, C.D. Pfeiffer, B.E. Richter, T.S. Stevens, J. High Resol. Chromatogr. Chromatogr. Commun. 10 (1987) 446.
[11] T. Tsuda, K. Nomura, G. Nakagawa, J. Chromatogr. 248 (1982) 241.
[12] G.J.M. Bruin, P.P.H. Tock, J.C. Kraak, H. Poppe, J. Chromatogr. 517 (1990) 557.
[13] Y. Guo, L.A. Colón, Anal. Chem. 67 (1995) 2511.
[14] C. Fujimoto, J. Kino, H. Sawada, J. Chromatogr. A 716 (1995) 107.
[15] C. Fujimoto, J.Y. Fujise, E. Matsuzawa, Anal. Chem. 68 (1996) 2753.
[16] C. Ericson, J. Liao, K. Nakazato, S. Hjerten, J. Chromatogr. A 767 (1997) 33.
[17] A. Palm, M.V. Novotny, Anal. Chem. 69 (1997) 4499.

[18] E.C. Peters, M. Petro, F. Svec, J.M. Fréhet, Anal. Chem. 69 (1997) 3646.
[19] E.C. Peters, M. Petro, F. Svec, J.M. Fréchet, Anal. Chem. 70 (1998) 2288.
[20] E.C. Peters, M. Petro, F. Svec, J.M. Fréchet, Anal. Chem. 70 (1998) 2296.
[21] S.M. Fields, Anal. Chem. 68 (1996) 2709.
[22] H. Minakuchi, K. Nakanishi, N. Soga, N. Ishizuka, N. Tanaka, Anal. Chem. 68 (1996) 3498.
[23] N. Ishizuka, H. Minakuchi, K. Nakanishi, N. Soga, K. Hosoya, N. Tanaka, J. High Resol. Chromatogr. 21 (1998) 477.
[24] J.G. Dorsey, A.S. Lister, P.B. Wright, S.C. Wendelke, T.L. Chester, Presented at the 19th International Symposium on Capillary Chromatography and Electrophoresis, Wintergreen, Virginia, USA, May, 1997.
[25] A. Malik, J.D. Hayes, D. Wang, S.L. Chong, G.S. Corbett, J.W. Cramer, Presented at the 19th International Symposium on Capillary Chromatography and Electrophoresis, Wintergreen, Virginia, USA, May, 1997.
[26] M.T. Dulay, R.P. Kulkarni, R.N. Zare, Anal. Chem. 70 (1998) 5103.
[27] R. Asiaie, X. Huang, D. Farnan, C. Horvath, J. Chromatogr. A 806 (1998) 251.
[28] T. Adam, K.K. Unger, M.M. Dittmann, G. Rozing, Presented at the 21st International Symposium on High Performance Liquid Phase Separations and Related Techniques. Birmingham, UK, June 1997.
[29] Q. Tang, Y. Shen, N. Wu, M.L. Lee, J. Microcol. Sep., in press.
[30] A. Malik, W. Li, M.L. Lee, J. Microcol. Sep. 5 (1993) 361.
[31] B. Xin, S.E. Tolley, M.L. Lee, Presented at the 19th International Symposium on Capillary Chromatography and Electrophoresis, Wintergreen, Virginia, USA, May, 1997.
[32] C.J. Brinker, G.W. Scherer, Sol–gel Science: The Physics and Chemistry of Sol–gel Processing, Academic Press, San Diego, CA, USA, 1990.
[33] J.D. Mackenzie, Hybrid Organic-Inorganic Composites, in: ACS Symposium Series 585, American Chemical Society, Washington, D.C., USA, 1995, pp. 227–236.
[34] J. Frick, Aerogels, Springer-Verlag, New York, USA, 1986.
[35] M. von Smoluchowski, Bull. Intern. Acad. Sci. Cracovie 1 (1903) 184.
[36] C.F. Poole, S.K. Poole, Chromatography Today, Elsevier, Amsterdam, 1991.